Assessing the Utility of a New Geophysical Subsurface Imaging System for Efficient Evaluation of Recharge Sites

Ahmad A. Behroozmand
Department of Geophysics, Stanford University
Stanford University
Stanford, California, USA
ahmad@vista-clara.com
Bio ▸

Esben Auken
Hydrogeophysics Group, Department of Geoscience,
Aarhus University
Aarhus, Denmark
esben.auken@geo.au.dk
Bio ▸

Rosemary Knight
Stanford University
Stanford, California, USA
rknight@stanford.edu
Bio ▸

Introduction

California has one of the largest agricultural industries in the United States, with irrigation of agricultural lands occurring from both surface water and groundwater. During drought periods, for instance over the past 10 years, the shortage of surface water supplies has led to extensive pumping of groundwater to meet irrigation needs. As a result, the groundwater level has declined in many of the groundwater basins in California. With passage of the Sustainable Groundwater Management Act (SGMA) in 2014, sustainable groundwater management has become a requirement in California with many water agencies now developing groundwater sustainability plans. In doing that, much attention is now focused on managed aquifer recharge (MAR) of the groundwater systems to improve our understanding of the controls on MAR, and to find new approaches to enhance the volume of recharge.

A common MAR approach is to direct storm water run-off during the winter months into a recharge pond, allowing the water to infiltrate below the pond and later be recovered for use. In the past few years, growers in the Central Valley of California have been exploring the use of on-farm recharge where excess surface water in the winter months is used to flood fields or groves. When assessing the suitability of a site for a MAR pond or for on-farm recharge, information about the subsurface materials and their hydraulic properties is critical. While poor infiltration leads to inefficiencies in a MAR pond, the consequences can be more serious when flooding groves or fields; ponding can damage trees or crops, and increase the risk of disease.

In the Central Valley of California the water table is typically at an intermediate depth interval (10s of meters). Soil maps are commonly used as a way to estimate a groundwater recharge suitability index (e.g. Soil Agricultural Groundwater Banking Index, SAGBI (O'Geen et al., 2015) or LandIQ (landiq.com)) but they do not provide information about the underlying material. Information about lithology can be obtained from the Central Valley Hydrologic Model, CVHM (Faunt, 2009). However, CVHM has spatial resolution on the order of ~ 1.6 km in the horizontal direction and ~ 15.2 m in the vertical direction. Neither of these approaches is optimal for assessing the suitability of a site for MAR.

When studying a potential MAR site in places like the Central Valley of California, it is important to use a method that is capable of characterizing subsurface materials in both the (relatively-thick) unsaturated and saturated zones. Other important criteria include fast coverage, efficiency and high resolution. A number of studies have shown the potential usefulness of geophysical methods to assess potential MAR sites. Different geophysical methods are sensitive to different physical parameters of the subsurface materials and also have their own limitations with respect to the area of coverage, penetration depth and spatial resolution. The objective of this study was to evaluate a new and efficient geophysical imaging method capable of providing the coverage and resolution that are optimal for the assessment of MAR sites in the Central Valley of California, where there is an interest in recharging both the shallow (<20 m) and intermediate (20 m to 50 m) parts of the groundwater system. This new method, a time-domain electromagnetic method (TEM), towed behind an all-terrain vehicle (ATV), and called tTEM (Auken et al., 2018), is an efficient way to acquire the data needed to model MAR at a site, can advance our ability to identify important areas for natural recharge, and can inform the selection of sites for MAR or on-farm recharge. Until recently, no geophysical surveying system has existed that is appropriate for assessing MAR sites, i.e. a system that is efficient and capable of 3D imaging of both shallow and intermediate depth intervals.

The tTEM system

The tTEM system uses a 2 m by 4 m single-turn coil as a transmitter and a multi-turn 0.5 m by 0.5 m coil with an effective area of 5 m^2 as a z-component receiver. The transmitter and receiver are separated by 9 m in an out-of-loop offset configuration. The electronic components are mounted on the back of an ATV and the system is towed behind the ATV while driving. Geographical position of the data is recorded continuously and the navigation and data collection are controlled by the driver/operator. Typical operation speed is ~ 15-20 km/h. The tTEM system is a dual-moment system using low and high moments to measure early and late time data that are used for shallow

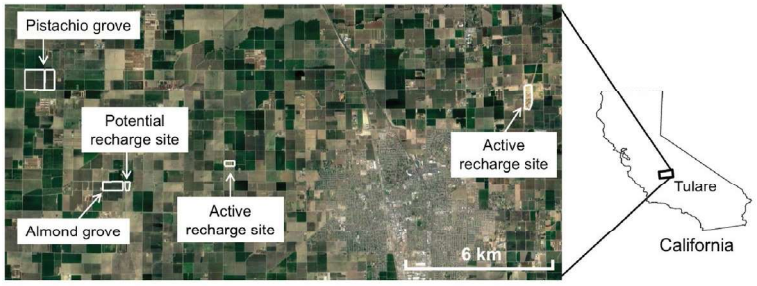

Figure 1. Location map of the study sites in the Tulare Irrigation District, California. The base map is taken from Google Earth.

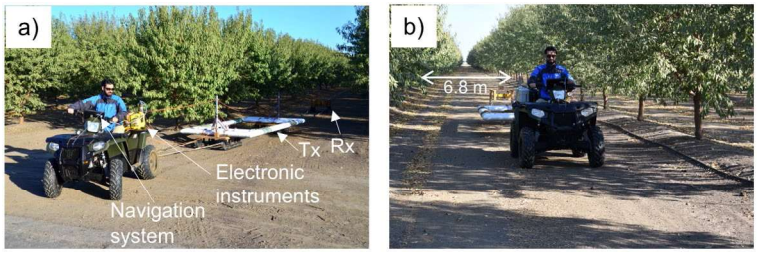

Figure 2. tTEM in operation at Site 1 (almond grove). Tree spacing is 6.8 m.

and deep investigations, respectively. Transmitter currents of ~ 2.8 A and ~ 30 A are used for low- and high-moment data. All details about the tTEM system specifications are presented in the paper by Auken et al. (2018).

The study area

Our field sites are located in the Tulare Irrigation District in the Central Valley of California. The location of the field sites is shown in Figure 1. Over a two-day period, we acquired ~ 92 line-km of data in two private properties where there is interest in on-farm recharge (one almond grove and one pistachio grove), one open field being considered as a new MAR basin, and two existing MAR basins. During this survey, the groves were last irrigated weeks before the tTEM survey, the open field had no crops so there would have been no irrigation, and the two existing MAR basins had no water. Therefore, we expected minimal saturation differences in the shallow subsurface between the sites.

Results

Detailed results from all study sites can be found in Behroozmand et al. (2019) but in this paper we limited ourselves to results from site 1.

Site 1 is a 400 m by 800 m almond grove. As shown in Figure 2, the tTEM system, ~2 m wide, fits perfectly between the rows of trees with their 6.8 m spacing. We covered the entire grove in ~ 6 hours, acquiring a total of 43 line-km of data. At this site, sounding data were acquired at every 2-2.5 m, and averaged during data processing, which led to datasets at every 10-12 m that were used for inversion. Figure 3 shows a 3D view of the resistivity model derived from the acquired data at Site 1. Warm colors (oranges and reds) correlate with high-resistivity units and cool colors (blues) correlate with low-resistivity

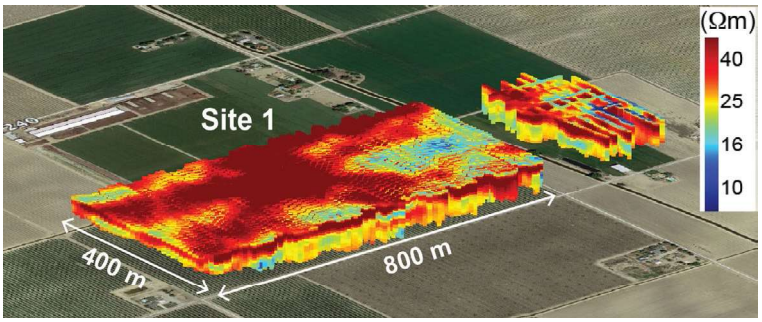

Figure 3. 3D views of the resistivity models from the acquired data at site 1.

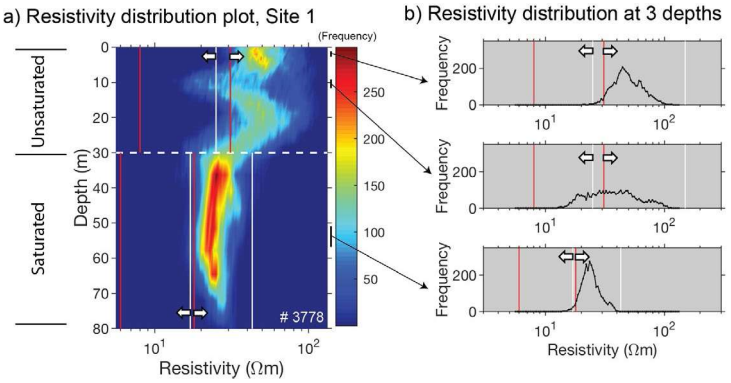

Figure 4. (a) Resistivity distribution plot of site 1. The white dashed line shows the saturated-unsaturated boundary. Red and white lines show clay and sand and gravel resistivity intervals obtained from the resistivity-lithology transform. Note that different resistivity-lithology models are considered in the saturated and unsaturated zones. Thick arrows indicate thresholds for clay, and sand and gravel resistivity values. The intervals between the thick arrows correspond to both clay, and sand and gravel. The total number of inverted resistivity models at this site is shown at the bottom-right corner of the plot. (b) Examples of resistivity distributions at three depth intervals. Note the variation in the range and width of the resistivity distributions.

units. A total of 3,778 inverted models, plotted next to each other in Figure 3, provide high-resolution 3D information of the subsurface.

Overall, noise conditions were good at the study sites and a good signal-to-noise ratio was obtained at each site. At each site, all acquired data were inverted together to obtain a model of electrical resistivity of the subsurface. We used a 30-layer smooth model and applied spatial constraints to the model parameters. A multi-layer model was chosen to better capture the complex geologic features at each site. The layer thickness started at 1 m at the top of each resistivity model and was increased by a factor of 1.1 down to the bottom of the model. The inverted models are displayed down to their depth of investigation (DOI; following Christiansen and Auken (2012)).

Given the dense data coverage provided by tTEM, we obtained detailed 3D structural information at each site. In addition, we used 'resistivity distribution plots' to evaluate the overall variations of lithology. The resistivity distribution plot of site 1 is shown in Figure 4a. This plot comprises all inverted resistivity models (here 3,778) at the site and contains the following information: (1) At each depth along the y-axis, a distribution of resistivities for the entire site is plotted on a logarithmic scale. Examples of resistivity distributions at three depth intervals are shown in Figure 4b. The shown location of the boundary between the unsaturated and saturated zone was determined through analysis of the distributions, described below. These

plots show how the range and width of resistivity distributions vary as a function of depth. (2) At each resistivity value along the x-axis, the color displays the number of models with that resistivity value. Therefore, warm colors indicate higher number of models with corresponding resistivity values. (3) Given a resistivity-lithology transform, corresponding ranges of resistivity values at each depth interval can be used to describe lithology as will be discussed later. (4) Each resistivity model on the resistivity distribution plot is terminated at its DOI. This, together with the number of models at each site (i.e. the color of the distribution) provides, at the bottom part of each plot, information about the DOI at each site.

To identify the subsurface lithology at each site, we used a resistivity-lithology transform developed in the study area. The transform was built using airborne EM data and lithologic (drillers') logs in the area. Each layer in the lithologic log had a described thickness and an assigned, simplified, lithology of either 1) sand and gravel, or 2) clay within the unsaturated zone, and of any 1) sand and gravel, 2) mixed fine and coarse, or 3) clay within the saturated zone. Separate transforms were built for unsaturated and saturated sediments. In addition, we assumed the absence of a capillary fringe and thus rapid saturation changes across the water table. Red and white lines in Figure 4a show "clay" and "sand and gravel" resistivity intervals obtained from the resistivity-lithology transform. The thick arrows indicate thresholds for sand and gravel, and clay resistivities. Detailed information about the resistivity-lithology transform are presented in Knight et al. (2018).

We used this resistivity-lithology model to interpret our resistivity distribution plots, but required information about the boundary between the saturated and unsaturated zone, given the impact of saturation on the resistivity transforms. We did not find available water level data useful for this study. Therefore, we developed an approach that would allow us to use the resistivity distributions to identify the saturated-unsaturated boundary. Our approach is based on two criteria. (1) Resistivity distribution collapse/broadening – when we consider the resistivity distribution plots, there is a collapse of the distribution (moving from top to bottom) or broadening of the distribution (moving from bottom to top) at a certain depth interval. This occurrence was used as a first indicator to define a saturated-unsaturated boundary, assuming that the groundwater table is parallel to the ground surface. Therefore, going from bottom to top we picked an interval where the distribution broadening occurred on the resistivity distribution plot. (2) Magnitude of resistivity values – following the resistivity-lithology model, we plotted the saturated zone clay, and sand and gravel resistivity intervals on top of the resistivity distribution plot, shown with red and white lines. Then we moved the saturated-unsaturated boundary (white dashed line) upward as long as there were no resistivity values greater than 43 ohm-m, which is the upper limit for resistivity of sand and gravel in the saturated zone. When a saturated-unsaturated boundary was set, a different set of lines was plotted above the boundary that indicate clay, and sand and gravel resistivity intervals in the unsaturated zone. Finally, we used those resistivity intervals to describe lithology.

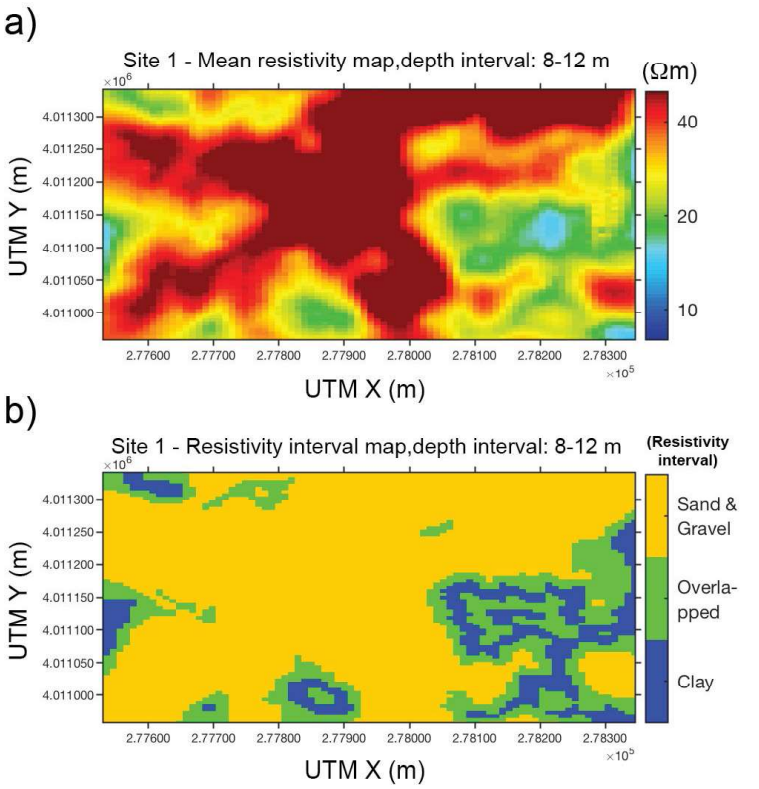

Figure 5. (a) A plan view map showing mean resistivity values at depth interval 8-12 m at site 1. (b) A similar map showing color-coded sand and gravel resistivity intervals (yellow), overlapped resistivity intervals (green) and clay resistivity intervals (blue), using the resistivity-lithology transform.

At site 1, we observe a clear broadening in the resistivity distribution at a depth of ~ 30 m, as shown in Figure 4a. We also observe that resistivity values larger than 43 ohm-m only occur above this depth. Therefore, this depth is considered to be the saturated-unsaturated boundary. In the saturated zone, nearly all resistivity values are larger than the sand and gravel threshold (shown with a thick arrow), which indicates coarse-grained sediments in the aquifer down to the DOI. Similarly, most resistivity values in the unsaturated zone are interpreted as sand and gravel. We observe a layer with a broad resistivity distribution at a depth interval of 8-12 m with values corresponding to both clay, and sand and gravel sediments. With respect to MAR, we conclude that this layer does not act as a hydraulic barrier. Most of the resistivity values in this layer correspond to sand and gravel. In addition, we see on a mean-resistivity plan view map at this depth interval that the clays are localized in a small portion of the site, as shown in Figure 5a. Figure 5b shows a similar map color-coded as sand and gravel resistivity intervals (yellow), overlapped resistivity intervals (green) and clay resistivity intervals (blue), using the resistivity interval values obtained from the resistivity-lithology model.

With this information, we conclude that site 1 is a good candidate for on-farm recharge and water is expected to infiltrate easily through the coarse sediments in the unsaturated zone.

The resistivity histograms obtained from the resistivity-lithology models of saturated and unsaturated zones consist of two intervals of resistivity values that can be interpreted, with a high degree of confidence, as 100% clay or 100% sand and gravel, and an overlap interval for which resistivity values can be

interpreted as either clay or sand and gravel. This information was used to create probability maps for different lithologic units. In addition, the resistivity distributions from the resistivity-lithology model can be used to create maps of the most probable lithologic unit at each site. This information is helpful in assessing a MAR site. Examples of most probable lithology sections can be found in Behroozmand et al. (2018).

Conclusions

We found that a new geophysical imaging system, tTEM, is ideally suited for assessing the suitability of MAR sites in the Central Valley of California. The tTEM system is efficient and provides a high-resolution 3D image of the subsurface down to a depth of greater than 60 m, allowing us to map out both unsaturated and saturated zones even in places where the groundwater level is relatively deep. The results of our two-day survey provided detailed resistivity models at seven study sites. The resistivity distribution plots were used to assign a saturated-unsaturated boundary at each site, allowing us to then use resistivity-lithology transforms to interpret the resistivity models in terms of lithology. The results of our study suggest that five of the seven sites are appropriate for MAR.

Acknowledgements

This project was funded by Stanford School of Earth, Energy and Environmental Sciences, and by the Center for Groundwater Evaluation and Management in the Stanford Geophysics Department (gemcenter.stanford.edu). We thank Aaron Fukuda of Tulare irrigation District for his great help that facilitated this research project and the landowners for access to their property.

References

Auken, E., A.V. Christiansen, C. Kirkegaard, G. Fiandaca, C. Schamper, A. Behroozmand, A. Binley, E. Nielsen, F. Effersø, N. Christensen, K, Sørensen, N. Foged and G. Vignoli, 2015. An overview of a highly versatile forward and stable inverse algorithm for airborne, ground-based and borehole electromagnetic and electric data. Explor. Geophys. 46(3): 223–235.

http://www.hgg.geo.au.dk/Papers_EndNote/3417748853/AUKEN2015.pdf

Auken, E., A. Christiansen, J. Westergaard, C. Kirkegaard, N. Foged and A. Viezzoli, 2009. An integrated processing scheme for high-resolution airborne electromagnetic surveys, the SkyTEM system. Explor. Geophys. 40(2): 184–192. doi: 10.1071/EG08128.

http://www.hgg.geo.au.dk/Papers_EndNote/1745956099/AUKEN2009.pdf

Auken, E., N. Foged, J. Larsen, K. Lassen, P. Maurya, S. Dath and T, Eiskjær, 2018. tTEM – a Towed TEM-system for Detailed 3D Imaging of the Top 70 meters of the Subsurface. GEOPHYSICS 84(1): 1–37. doi: 10.1190/geo2018-0355.1.

http://www.hgg.geo.au.dk/Papers_EndNote/1717665328/tTEM2018.pdf

Behroozmand, A.A., E. Auken, and R. Knight. 2019. Assessment of managed aquifer recharge sites using a new geophysical imaging method. Vadose Zone J. 18:180184.

https://dl.sciencesocieties.org/publications/vzj/pdfs/18/1/180184

Faunt, C. 2009. Groundwater Availability of the Central Valley Aquifer, California.

https://pubs.usgs.gov/pp/1766/

https://ca.water.usgs.gov/projects/central-valley/central-valley-groundwater-availability.html

Knight, R., R. Smith, T. Asch, J. Abraham, J. Cannia, A. Viezzoli and G. Fogg, 2018. Mapping Aquifer Systems with Airborne Electromagnetics in the Central Valley of California. Groundwater 56(6), 893-908. doi: 10.1111/gwat.12656.

https://ngwa.onlinelibrary.wiley.com/doi/full/10.1111/gwat.12656

O'Geen, A., M. Saal, H. Dahlke, D. Doll, R. Elkins, A. Fulton, G. Fogg, T. Harter, J. Hopmans, C. Ingels, F. Niederholzer, S, Solis and P. Verdegaal. 2015. Soil suitability index identifies potential areas for groundwater banking on agricultural lands. Calif. Agric. 69(2): 75–84.

http://calag.ucanr.edu/Archive/?article=ca.v069n02p75

Vest Christiansen, A., and E. Auken. 2012. A global measure for depth of investigation. GEOPHYSICS 77(4): WB171–WB177. doi: 10.1190/geo2011-0393.1.

http://www.hgg.geo.au.dk/Papers_EndNote/0039019423/CHRISTIANSEN2012.pdf

Viezzoli, A., A. Christiansen, E. Auken, and K. Sørensen. 2008. Quasi-3D modeling of airborne TEM data by spatially constrained inversion. GEOPHYSICS 73(3): F105–F113. doi: 10.1190/1.2895521.

http://www.hgg.geo.au.dk/Papers_EndNote/0691047853/Viezzoli2008.pdf

Author Bios

Ahmad A. Behroozmand
Department of Geophysics, Stanford University
Stanford, CA 94305, USA
ahmad@vista-clara.com

Ahmad Ali Behroozmand is a Senior Geophysicist with Vista Clara Inc. He has a PhD degree in Geophysics from Aarhus University, Denmark, and specializes in the development and application of geophysical methods for subsurface investigations, with a focus on hydrogeological problems.

Esben Auken
Hydrogeophysics Group,
Aarhus University, Aarhus, Denmark
esben.auken@geo.au.dk

Esben Auken is a Professor at the Hydrogeophysics Group, Aarhus University, Denmark. He and Associate Prof. Anders Vest Christiansen heads the research group which is around 20 people. He research interests is focused around high resolution geophysics for hydrological and geotechnical applications. The research group develops geophysical instrumentation, data processing and inversion algorithms and statistical with methods for efficient usage of the geophysical models in groundwater resource models. He holds several board positions and has created not less than three spin-off companies during the last decay.

Rosemary Knight
Stanford University
Stanford, California, USA
rknight@stanford.edu

Rosemary Knight received a B.Sc. and M.Sc. in Geological Sciences from Queen's University, Canada and a Ph.D. in Geophysics from Stanford University, U.S.A. She was on the faculty at the University of British Columbia, Vancouver, Canada for 13 years, returning to Stanford in 2000. She is currently the George L. Harrington Professor of Earth Sciences in the Department of Geophysics at Stanford. Her current research includes laboratory, theoretical and field studies related to the use of geophysical methods for subsurface imaging. She is the founding director of the Center for Groundwater Evaluation and Management (GEM Center) (gemcenter.stanford.edu) – a research initiative to develop and demonstrate news ways of using geophysical methods for groundwater applications. Rosemary recently served as the David Keith Todd Distinguished Lecturer for Groundwater Resources Association of California (GRA), and also recently received the GRA Kevin J. Neese Award given to the GEM Center, in recognition for their groundbreaking research and application of Geophysics to the evaluation and management of groundwater resources.